

## An MNDO SCF-MO Study of the Mechanism of the Cannizzaro Reaction

Henry S. Rzepa\* and Jonathan Miller

Department of Chemistry, Imperial College of Science and Technology, London SW7 2AY

The mechanism of the Cannizzaro reaction has been studied using the MNDO SCF-MO method. A hydride transfer between the intermediate (1) to the aldehyde (2) ( $R = R^1 = H$ ) was calculated to proceed *via* a symmetrical transition state with a barrier of 72 kJ mol<sup>-1</sup>. Alternative mechanisms involving a single-electron transfer between (1) and (2) are predicted to be less favourable, particularly for aliphatic aldehydes. A radical chain mechanism involving a single-electron-transfer step is proposed as an alternative. Mechanisms involving dianions are discussed, in which single-electron transfers are particularly favourable, and radicals such as H<sup>•</sup> should be formed at high pH. Primary hydrogen kinetic isotope effects are calculated for all the steps involving hydrogen transfers and the results discussed in terms of the symmetry and properties of the transition states.

The Cannizzaro reaction involves the base-catalysed disproportionation of an aldehyde devoid of  $\alpha$ -hydrogens to the corresponding carboxylic acid and alcohol.<sup>1</sup> Prior to the advent of metal hydrides as synthetic reagents, this was considered to be one of the most fundamental reactions in organic chemistry.<sup>1</sup> In 1931 Haber and Willstätter<sup>2</sup> proposed that this reaction proceeds by a radical chain mechanism initiated by a single-electron transfer (SET), but this has since been discounted on the basis that neither radical initiators nor inhibitors have a decisive effect on the rate of reaction.<sup>3</sup> Numerous subsequent investigations<sup>4</sup> appeared to establish firmly the rate-limiting step in this mechanism as involving a hydride transfer from the initially formed intermediate (1) to a second molecule of aldehyde [Figure 1, path (a)]. However, the measured primary kinetic isotope effects are unusually low for a hydrogen-transfer reaction.<sup>4</sup> Very recently, Chung<sup>5</sup> has studied the disproportionation of [ $\alpha$ -<sup>2</sup>H]benzaldehyde in alkaline aqueous dioxane, finding that only 80% of the product was [ $\alpha$ -<sup>2</sup>H<sub>2</sub>]benzyl alcohol, the remainder being monodeuterated. The <sup>1</sup>H impurity was suggested to arise from the solvent *via* abstraction by radical intermediates. The presence of aldehyde radical anions under reaction conditions appropriate for the Cannizzaro reaction has subsequently been demonstrated by e.s.r. spectroscopy.<sup>6</sup> These results have led to an alternative mechanism being suggested<sup>5,6</sup> [Figure 1, path (b)] based on a single-electron transfer (SET) between the intermediate (1) and the aldehyde (2). However, the proportion of reaction proceeding by this pathway is not known, nor is there any indication of whether this mechanism is consistent with the observed isotope effects.

We report in this paper a theoretical examination of the Cannizzaro reaction, using the MNDO SCF-MO procedure.<sup>7</sup> This method has been extensively applied to the study of reaction surfaces and has been shown to satisfactorily reproduce the properties of various hydrogen-transfer reactions.<sup>8</sup>

### Computational Procedure

The calculations were carried out using the standard MNDO procedure<sup>7</sup> with full optimisation of all geometric variables, using the spin-restricted (RHF) SCF procedure for closed-shell systems and the spin-unrestricted (UHF) SCF procedure for open-shell systems.<sup>9</sup> All doublet and triplet states calculated using this method showed little higher spin contamination ( $\langle S^2 \rangle \leq 0.8$  for doublets and  $\leq 2.1$  for triplets). Ground-state radical pairs were also calculated using the spin-unrestricted procedure,<sup>9</sup> for which  $\langle S^2 \rangle$  ca. 1.0 in most cases. Transition states for hydrogen transfer were initially located by calculating

the energy of the system as a function of the two C-H bond lengths involved and locating an approximate saddle point from a contour map. These points were then refined by minimising the sum of the squared scalar gradients<sup>10</sup> and characterised as transition states by calculating the force-constant matrix<sup>11</sup> and showing that this had only one negative eigenvalue with the correspondingly correct displacement coordinates. Normal vibrational frequencies obtained from the force-constant matrix were used with the standard harmonic-oscillator model<sup>8</sup> to obtain kinetic isotope effects for these reactions. The calculated vibrational frequencies for all the isotopic species, and the components of the partition function ratios are given in Supplementary Publication No. SUP 56193 (14 pp.).† All calculations refer to the substituents  $R = R^1 = H$  except where noted otherwise.

### Results and Discussion

1. *Hydride-transfer Mechanism* [Figure 1, path (a)].—The first step in this mechanism involves a pre-equilibrium between hydroxyl ion and (2) to form the intermediate (1). Since CH bonds  $\alpha$  to an alkoxide substituent have been shown<sup>12</sup> to be substantially weaker than normal C-H bonds, (1) might be expected to undergo relatively facile hydrogen-transfer reactions. Activation energies ranging from 72 to 90 kJ mol<sup>-1</sup> have indeed been reported for such intramolecular hydride-transfer reactions to a carbonyl group.<sup>13</sup>

In studying this reaction using the MNDO procedure<sup>7</sup> we initially calculated the energies of the reactants (1 and 2), the intermediates (3 and 4) and the products (5 and 6) separately. However, when each pair was treated as a single molecule, intermolecular stabilisation energies of 42, 48, and 47 kJ mol<sup>-1</sup>, respectively, were obtained, corresponding to the formation of fairly strong hydrogen bonds. A transition state (t.s.) (7) for H<sup>-</sup> transfer was located from the energy-contour map (Figure 2) constructed using the C-H bond lengths as reaction coordinates. The calculated activation energy (72 kJ mol<sup>-1</sup>) is similar to the experimental values noted above<sup>13</sup> and the transition state corresponds to a symmetrical hydrogen transfer in which the nuclear and electronic components are effectively synchronous [Figure 3(a)]. The calculated charge on the hydrogen being transferred (-0.30) is similar to that estimated by Kreevoy (-0.23) on the basis of kinetic evidence for a related hydride-transfer reaction.<sup>14</sup> The Cannizzaro reaction is completed by a proton transfer, which in protic media certainly

† For details of the Supplementary Publications Scheme see Instructions for Authors, *J. Chem. Soc., Perkin Trans. 2*, 1985, Issue 1.

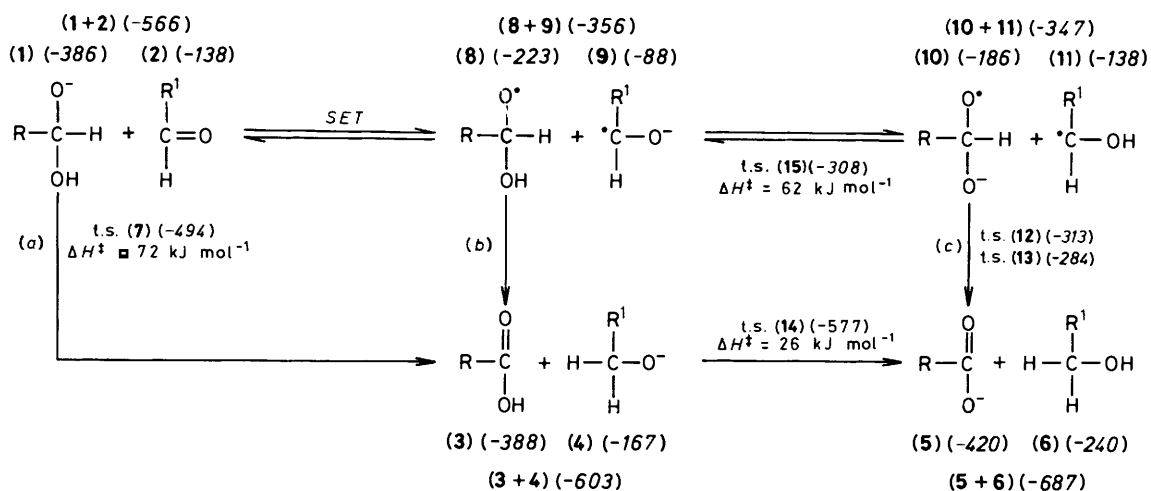


**Figure 1.** The mechanism of the Cannizzaro reaction proceeding *via* (a) a hydride transfer and (b) and (c) a single-electron transfer. Values in parentheses represent the MNDO-calculated standard enthalpies of formation, in  $\text{kJ mol}^{-1}$ .

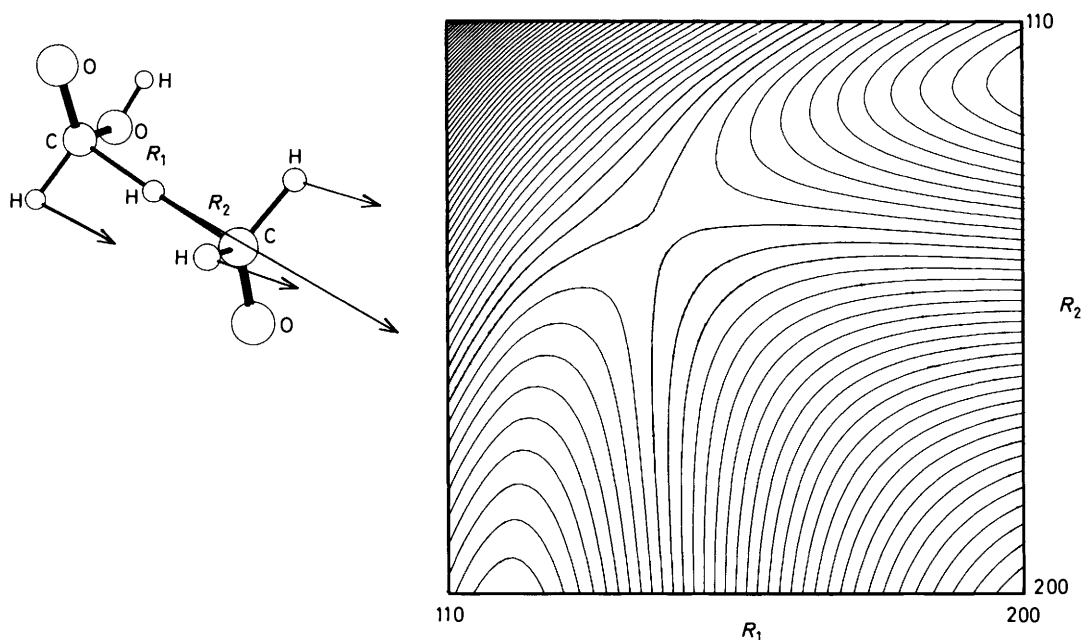


**Figure 2.** Contour map showing the calculated energy of (1) and (2) as a function of the two reaction co-ordinates  $R_1$  and  $R_2$ . The contour separation is  $4.18 \text{ kJ mol}^{-1}$ , bond lengths in pm

corresponds to an intermolecular process. The MNDO method predicts an intramolecular transfer to proceed *via* a transition state (14) [Figure 3(b)] with a relatively small barrier, even though no allowance for solvation has been made.

The calculated effects of R or  $R^1 = F$ , which is a strong  $\sigma$ -accepting and  $\pi$ -donating substituent, are shown in Table 1. The substitution R = F decreases the H-donor ability of (1) by the  $\sigma$ -inductive effect and the reaction proceeds *via* a late transition state whereas with  $R^1 = F$  the electrophilic properties of (2) are enhanced and an early transition state results. When both R =  $R^1 = F$ , the substituent on (1) appears to dominate, and the effect is to produce a significantly 'looser' transition state than with no substitution. The overall effect of direct fluorine substitution is to increase rather than to decrease the activation energy for a hydride transfer. Experimental evidence indicates, however, that electron-withdrawing substituents on a phenyl

group increase the rate of reaction of aromatic aldehydes<sup>4</sup> ( $p + 3.76$ ). This may indicate that the  $\pi$ -mesomeric effect on the electrophilic properties of the carbonyl group is more important in aromatic systems, or indeed that in such systems there may be significant contribution from alternative mechanisms.

We also investigated the possibility that the hydride- and proton-transfer steps in path (a) could be telescoped into one cyclic transition state.<sup>4</sup> Although we were unable to locate a stationary point corresponding to this process, the related reaction of methanol with formaldehyde proceeding *via* a cyclic transition state was calculated to require an activation energy of  $365 \text{ kJ mol}^{-1}$ . Such high barriers are not surprising given the considerable necessary distortion from linearity of the three centres involved in the hydrogen transfer.

Since the Cannizzaro reaction is normally carried out in fairly polar solvents, the effect of the successive addition of two water

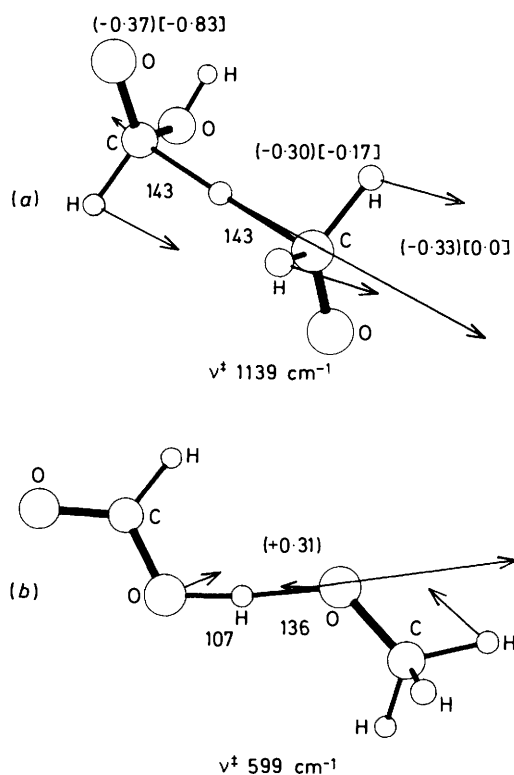


**Figure 3.** Calculated properties of the transition states (a) (7,  $R = R^1 = H$ ) and (b) (14). Bond lengths are shown in pm. The displacement coordinates corresponding to the reaction co-ordinate are indicated with arrows. The calculated atomic charges are shown in parentheses for the transition state and in brackets for the reactant

**Table 1.** Calculated MNDO properties of species involved in the hydride-transfer mechanism [path (a)] for the Cannizzaro reaction

R	R <sup>1</sup>	(1 + 2)	(7)	(3 + 4)	(5 + 6)
H	H	0 <sup>a</sup> (-566) <sup>b</sup>	72 <sup>a</sup> (143, 143) <sup>c</sup>	-37 <sup>a</sup>	-121 <sup>a</sup>
F	H	0 (-850) <sup>b</sup>	123 (157, 135) <sup>c</sup>	40	-135
H	F	0 (-820) <sup>b</sup>	81 (139, 150) <sup>c</sup>	-25	-92
F	F	0 (-1 099) <sup>b</sup>	126 (150, 142) <sup>c</sup>	22	-97

<sup>a</sup> Calculated energy (in kJ mol<sup>-1</sup>) relative to the reactant complex (1 + 2). <sup>b</sup> Calculated heat of formation, in kJ mol<sup>-1</sup>. <sup>c</sup> Calculated values for the reaction co-ordinates  $R_1$  and  $R_2$  (cf. Figure 2), in pm.

molecules was investigated. Their position relative to the other components was fully optimised in both the reactant and the transition state, and in both cases the water molecule was calculated to adopt a bridging position in the transition state (Figure 4). Each such molecule was calculated to stabilise the reactant, transition state, and products by a similar amount (Table 2), resulting in activation energies for the hydride transfer that are essentially similar to the unsolvated reaction. Although the inclusion of two water molecules does not by any means represent a full model of solvation, these results do provide some indication that neither the structures of the transition states nor the activation energies are greatly influenced by the presence of such a polar molecule.

2. *Single-electron-transfer Mechanism* [Figure 1, path (b or c)].—The mechanism as proposed by Chung<sup>5</sup> and Ashby<sup>6</sup>

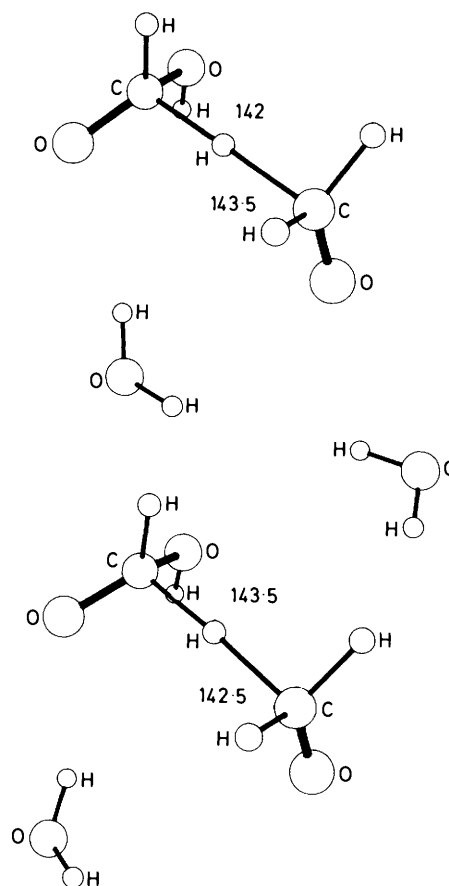


**Figure 4.** Calculated structures for (7,  $R = R^1 = H$ ) with the inclusion of one and two water molecules

**Table 2.** Calculated energies of species involved in the hydride-transfer mechanism [path (a)] with the inclusion of one and two water molecules

No. of water molecules	(1 + 2)	(7)	(3 + 4)
0	0 <sup>a</sup> (-566) <sup>b</sup>	72 <sup>a</sup>	-37 <sup>a</sup>
1	-23 (-844)	53	-58
2	-45 (-1 121)	37	-67

<sup>a</sup> Calculated energy (in kJ mol<sup>-1</sup>) relative to the reactant complex (1 + 2) and the relevant number of water molecules. <sup>b</sup> Calculated heat of formation, in kJ mol<sup>-1</sup>.

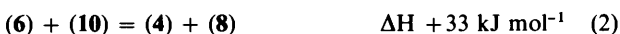
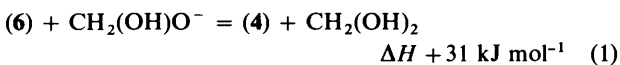
[Figure 1, path (b)] assumes the formation of the intermediate (1), followed by an electron transfer from (1) to (2) to give the radicals (8) and (9). A hydrogen-atom transfer between these species is then followed by a fast proton transfer to complete the reaction. A hitherto unconsidered alternative is that a proton transfer between (8) and (9) precedes the hydrogen-atom transfer [Figure 1, path (c)].

(i) *Path (b)*. A single-electron transfer between (1) and (2) corresponds to a first excited radical pair state of these species. In order to estimate the energy of this state using the spin-unrestricted (UHF) procedure, a triplet-state calculation has to be carried out, since in the absence of symmetry a UHF singlet calculation gives only a ground-state wavefunction. Since the products (8) and (9) are well separated, it is probable that the energies of the first excited singlet and triplet states will be

similar. It was possible to verify this assumption for the species (10) and (11), since the open-shell singlet radical pair is also the ground state and can in fact be calculated using the UHF method. The calculated charge distribution for the triplet state of (8) and (9) correctly corresponded to complete transfer of an electron from (1) to (2). The calculated heat of formation is 211 kJ mol<sup>-1</sup> higher than the ground-state complex between (1) and (2) and corresponds to an intermolecular stabilisation of 45 kJ mol<sup>-1</sup> between (8) and (9) (Figure 1). The relative energies of the closed-shell singlet and the open-shell triplet states are in effect a measure of the relative electron affinities of (1) and (2), and we note in this context that the MNDO method has been shown to predict with reasonable reliability such properties.<sup>15</sup> The spin-unrestricted (UHF) method used here is known<sup>9</sup> however to predict the energies of doublet and triplet states to be too low relative to closed-shell singlets, and so unless (8) and (9) are preferentially solvated compared with (1) and (2), the value of 211 kJ mol<sup>-1</sup> must represent a *lower* bound on the energy of the single-electron transfer. With R = R<sup>1</sup> = Ph, the triplet state ( $\Delta H$  -284 kJ mol<sup>-1</sup>) was calculated to be only 81 kJ mol<sup>-1</sup> higher than the singlet state, whereas the calculated activation energy for H<sup>-</sup> transfer (114 kJ mol<sup>-1</sup>) is higher than for R = R<sup>1</sup> = H. This suggests that for aromatic aldehydes undergoing the Cannizzaro reaction, the single-electron transfer and the H<sup>-</sup> transfer mechanisms are highly competitive, unlike aliphatic aldehydes where they are not. With R = R<sup>1</sup> = F, the triplet state is 253 kJ mol<sup>-1</sup> above the ground state of (1 + 2), which indicates that the electron-donor ability of (1, R = F) is inhibited more than the electron-acceptor properties of (2, R<sup>1</sup> = F) are enhanced. For such a system, the electron transfer to (2) is more likely to occur from a donor other than (1).

The next step, a hydrogen-atom transfer between (8) and (9) to give (3) and (4), must certainly involve an inter-system crossing between the first excited singlet and ground-state singlet surfaces. Such a process cannot be studied using the UHF method, but it should be noted that any additional barrier to such a hydrogen transfer can only render this pathway even less favourable energetically.

(ii) *Path (c)*. In considering this pathway, some discussion of the relative acidities of the species involved is relevant. It is known that the pK<sub>a</sub> of CH<sub>2</sub>(OH)<sub>2</sub> (13.3)<sup>16</sup> is significantly less than that of methanol (15.5)<sup>16</sup> due to the inductive effect of the second OH group. In order to estimate the corresponding substituent effects of an alkoxy radical [*cf.* (8)] and a radical centre itself [*cf.* (11)], we calculated  $\Delta H$  for the four equilibria (1)–(4). These results (which neglect any intermolecular inter-



actions, *cf.* Figure 1) indicate that the inductive effect of an O<sup>-</sup> group is slightly greater than that of an OH group (equations 1 and 2), whilst that of a radical centre itself is less (equations 1 and 3). In terms of pK<sub>a</sub> values, that of (8) is likely to be very similar to that of CH<sub>2</sub>(OH)<sub>2</sub> (*ca.* 13), whilst that of (11) is likely to be more similar to that of methanol itself (*ca.* 15). The equilibrium in equation (4) is therefore predicted to result in the formation of significant concentrations of (10) and (11).

The intramolecular proton transfer [15, Figure 5(a)] between (8) and (9) was studied on the triplet SCF surface and proceeds *via* a symmetrical transition state. This should be contrasted with the corresponding early and unsymmetrical transition

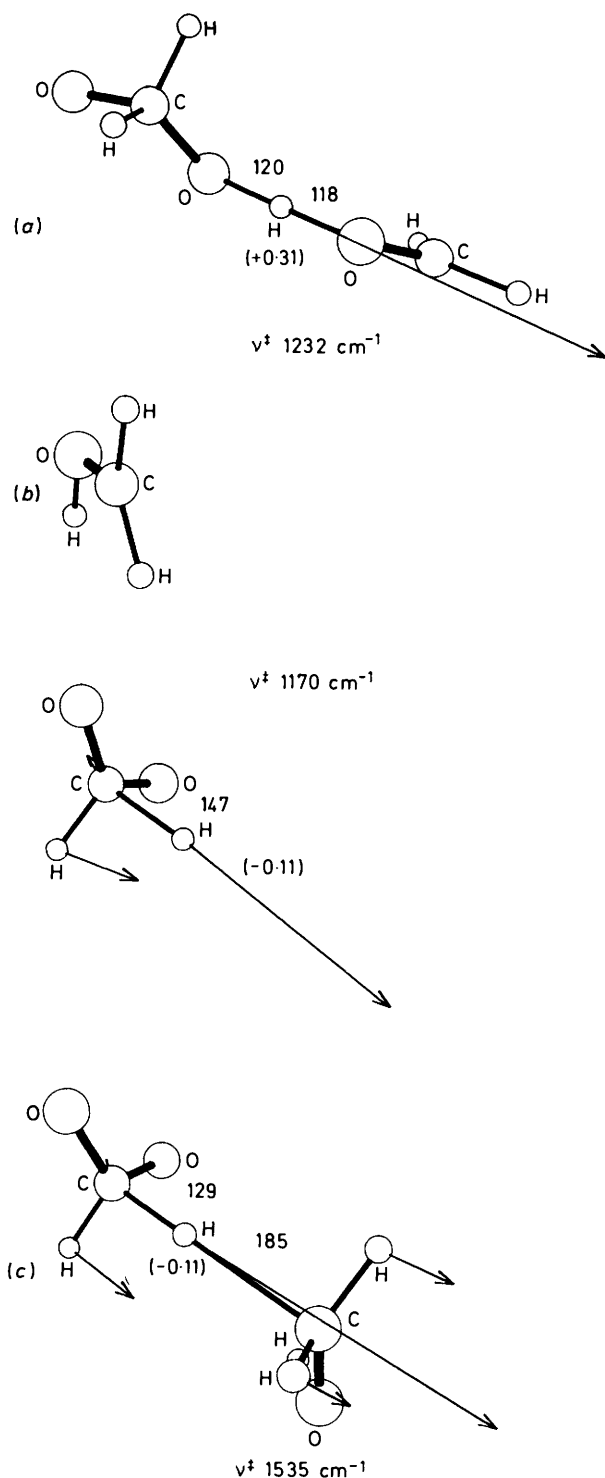
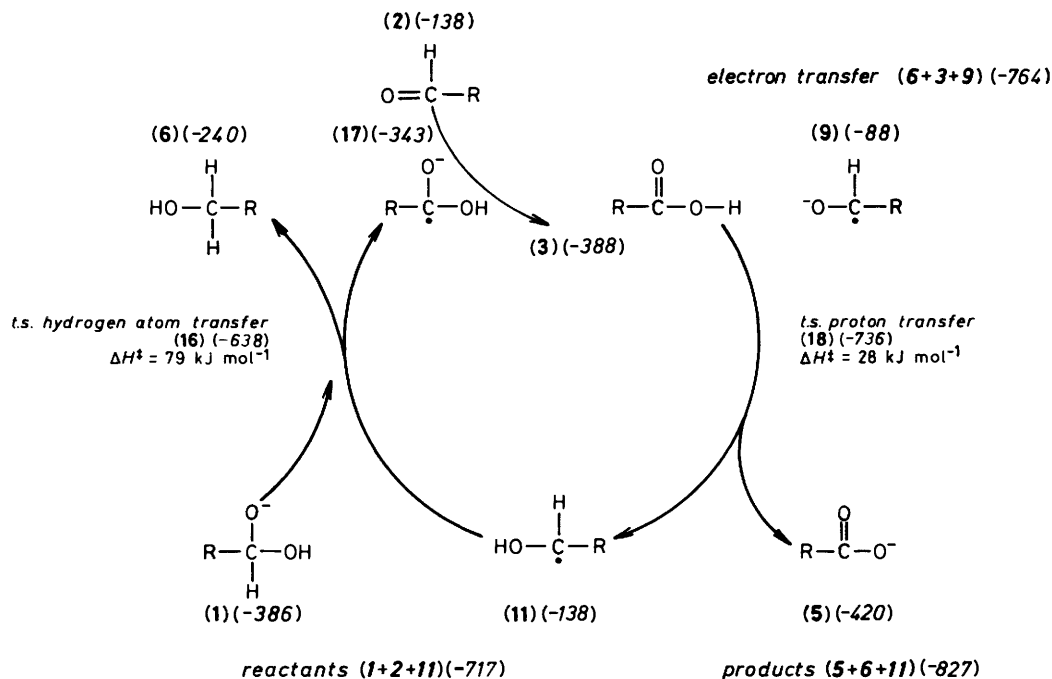


Figure 5. Calculated structures and charges for (a) (15), (b) (12), and (c) (13)

state for proton transfer between (3) and (4) [Figure 3(b)]. A hydrogen-atom transfer between (10) and (11) can proceed *via* two pathways. The first [12, Figure 5(b)] corresponds to homolysis of the C–H bond in (10) to give a ‘caged’ hydrogen atom, which can then combine with (11), and the second [13, Figure 5(c)] is a concerted transfer. The calculated barriers (34 and 63 kJ mol<sup>-1</sup>, using the UHF singlet method) are probably too high, since this method is known to overestimate barriers to reactions between radical pairs.<sup>9</sup> The overall conclusion for



**Figure 6.** Single-electron transfer-radical chain mechanism for the Cannizzaro reaction. Calculated heats of formation are shown in parentheses ( $\text{kJ mol}^{-1}$ )

both paths (b) and (c) is that they are unlikely to be favoured for aliphatic systems, and that even for aromatic aldehydes, other pathways are certainly competitive. The detection of intermediates such as (9) under Cannizzaro conditions<sup>6</sup> does not contradict this conclusion, since this species could arise by electron transfer not from (1) but from another electron donor. It was noted above that the inductive effect of an OH group increases the acidity of a neighbouring OH group, and likewise, the electron affinity of an alkoxy radical  $\text{O}^\cdot$  should be increased by the presence of such an OH group. It follows that the ability of (1) to act as a one-electron donor (especially when substituted with *e.g.*,  $\text{R} = \text{F}$ ) should be *less* than that of (4), or indeed that of hydroxy anion itself, both of which could transfer an electron to (2) to give (9).

**3. The Single-electron Transfer-Radical Chain Mechanism (Figure 6).**—As suggested above, a radical such as (9) could arise by a single-electron transfer from several donors, and at a pH of  $\leq 15$  it would be expected to protonate to give (11). The rate-determining step in this chain mechanism then involves hydrogen-atom abstraction from the intermediate (1) by the radical (11), which implies a kinetic second order with respect to the concentration of aldehyde. Intermolecular interactions between (1 + 2 + 11) and (6 + 3 + 9) of 55 and 48  $\text{kJ mol}^{-1}$ , respectively, are similar to those calculated previously (Figure 6). The hydrogen-atom transfer proceeds *via* transition state (16) with a calculated activation energy of 79  $\text{kJ mol}^{-1}$ , which is very similar to the value calculated for the hydride-transfer mechanism. The lengths of the two C-H bonds are very dissimilar [Figure 7(a)], corresponding to an early transition state. The significance of this in relation to the expected kinetic isotope effects is discussed later. At some point following the transition state, an electron transfer occurs between the initially formed product (17) and a further molecule of (2) to form (3) and (9). It is unlikely that (17) would have any significant lifetime. A low-energy proton transfer from (3) to (9) completes the chain, proceeding *via* transition state (18) [Figure 7(b)] in which the asymmetry of the transition state is also quite pronounced. As

noted above, in protic media this step is likely to involve a prototropic equilibrium with the solvent, and may lead to a complex kinetic order for the base concentration. Each step in the chain is calculated to be exothermic, and the overall heat of reaction is  $-110 \text{ kJ mol}^{-1}$ .

The calculated strong intermolecular interactions would render this a significantly 'caged' process, for which the entropy of activation might be expected to be less positive than for a normal bimolecular reaction. The lack of a decisive role by radical inhibitors could be explained by their having to disrupt these strong hydrogen bonds in order to have an effect. This mechanism requires that (9) be protonated to give a significant concentration of (11), which as discussed above, is quite probable in the pH region of 13.5–14.5 commonly encountered in Cannizzaro reactions. In the recent e.s.r. study<sup>6</sup> no evidence for a species such as (11) was reported, but this does not of course exclude its presence.

The possibility was considered that a hydrogen-atom transfer might occur directly between (9) and (1). A concerted transition state (19) was indeed located [Figure 7(c)], but the calculated activation energy (446  $\text{kJ mol}^{-1}$ ) excludes such a mechanism. This high value arises from the electrostatic repulsion of two negative ions. An alternative route that avoids this repulsion corresponds to a 'dissociative' mechanism, in which (1) fragments to give (17) and  $\text{H}^\cdot$ , followed by rapid combination of the  $\text{H}^\cdot$  with (9) to give (4). However, the homolysis of (1) to give free  $\text{H}^\cdot$  is calculated to require an activation energy of 261  $\text{kJ mol}^{-1}$ , and renders this pathway also unlikely.

**4. The Dianion Mechanism.**—In very strong base, it becomes possible for the intermediate (1) to be deprotonated to the dianion (20).<sup>4</sup> The kinetics of the Cannizzaro reaction involving formaldehyde for example, show a second-order dependence on  $[\text{OH}^-]$  under certain conditions.<sup>4</sup> In contrast to the mono-anion (1), a single-electron transfer from (20) to (2) is calculated to be highly exothermic (395  $\text{kJ mol}^{-1}$ ), resulting in the formation of the radical anions (10) and (9). As noted above, (10) is more likely to arise by electron transfer from (1) followed by

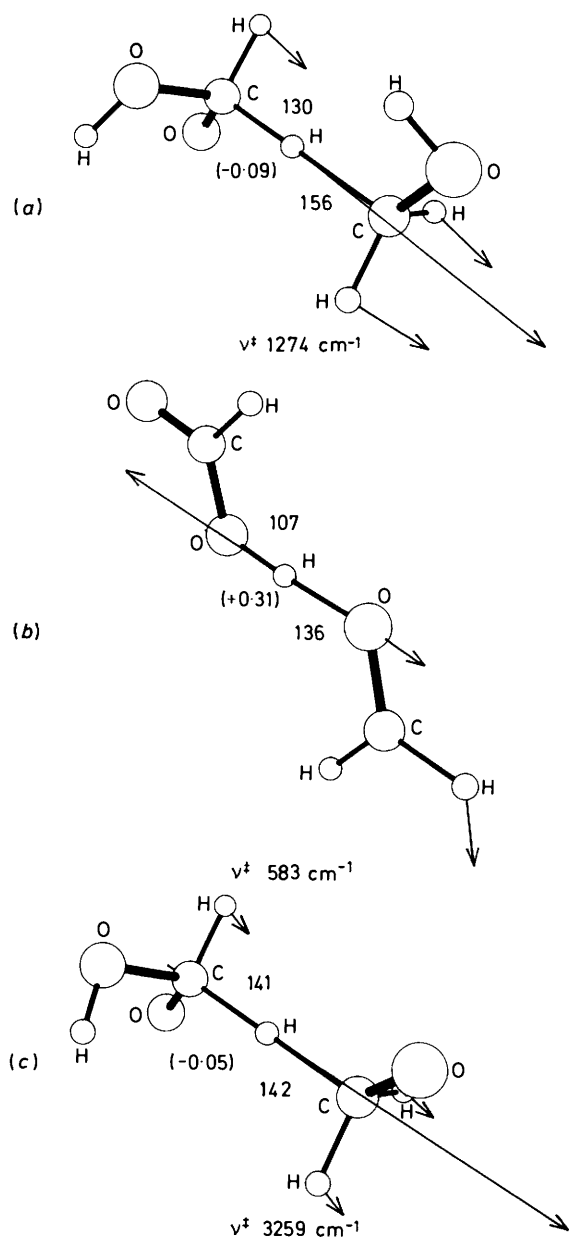


Figure 7. Calculated structures and atomic charges for (a) (16), (b) (18), and (c) (19)

deprotonation, rather than by initial deprotonation of (1). Under strongly basic conditions however, (9) is unlikely to protonate to give (11). A concerted pathway for direct hydrogen-atom transfer between (10) and (9) [Figure 8(a)] was found to involve a highly unsymmetrical transition state (21) with a very high activation energy (312 kJ mol<sup>-1</sup>). This is again due to the repulsion between the two negatively charged species. A dissociative pathway, involving the formation of (5) and H<sup>•</sup> from (10), was calculated to proceed *via* transition state (22) with an activation energy of 31 kJ mol<sup>-1</sup> [Figure 8(b)]. Combination of H<sup>•</sup> with (9) proceeds with no barrier.

Under strongly basic conditions therefore, we predict that both (9) and (10) will form, and if not protonated, the latter will fragment to give free hydrogen atoms.

**Hydrogen Kinetic Isotope Effects.**—Kinetic isotope effects provide one means of distinguishing between the various

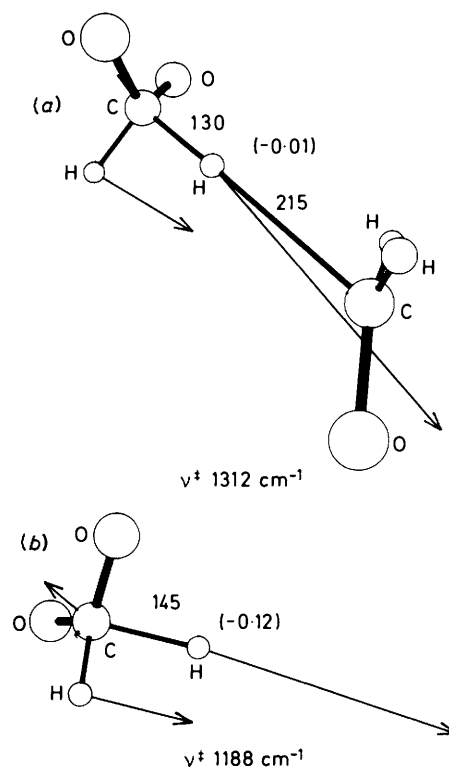


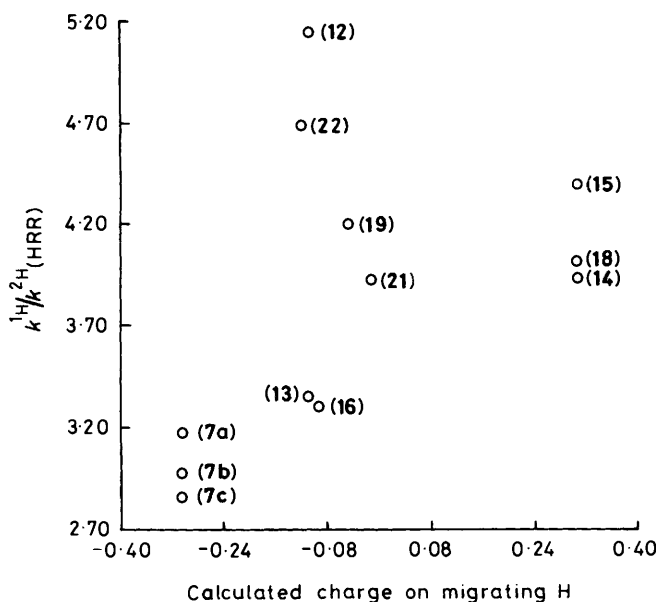
Figure 8. Calculated structures and atomic charges for (a) (21) and (b) (22)

Table 3. Calculated MNDO harmonic rate ratios for transition states involving hydrogen transfers, at 373 K

Transition state	$\nu_H^\ddagger/\nu_D^\ddagger$ <sup>a</sup>	VP <sup>a</sup>	EXC <sup>a</sup>	ZPE <sup>a</sup>	HRR <sup>a</sup>
(7, R = R <sup>1</sup> = H)	1.211	0.857	1.017	2.824	2.980
(7, R = F, R <sup>1</sup> = H)	1.166	0.881	0.965	3.208	3.177
(7, R = H, R <sup>1</sup> = F)	1.199	0.868	1.035	2.656	2.864
(14)	1.156	0.885	1.074	3.572	3.927
(15)	1.371	0.737	1.087	4.010	4.404
(12)	1.217	0.907	0.784	5.944	5.144
(13)	1.197	0.939	0.923	3.240	3.358
(16)	1.237	0.911	0.947	3.106	3.312
(18)	1.161	0.879	1.078	3.658	4.024
(19)	1.362	0.840	0.948	3.877	4.203
(21)	1.238	0.913	0.910	3.832	3.941
(22)	1.205	0.797	0.920	5.308	4.689

<sup>a</sup> Terms defined in reference 8.

proposed mechanisms. There have been several reports of both <sup>1</sup>H-<sup>2</sup>H and <sup>1</sup>H-<sup>3</sup>H isotope effects for Cannizzaro reactions of aromatic aldehydes, which appear to indicate unusually low values.<sup>4</sup> No variable-temperature study appears to have been carried out. Since the calculation of harmonic rate ratios<sup>8</sup> requires only the normal vibrational frequencies of both reactants and transition states, we have used these to calculate the <sup>1</sup>H-<sup>2</sup>H rate ratios for all the hydrogen transfers reported above. These results also represent an interesting test of Westheimer's proposal<sup>17</sup> that the magnitude of primary hydrogen isotope effects is directly related to the symmetry of the transition state. The results (Table 3) shows that both the magnitudes and the trends in the harmonic rate ratios (HRR) are dominated by the zero-point energy (ZPE) terms. A comparison of the effects of fluorine substitution on (7) shows



**Figure 9.** Calculated harmonic rate ratios (HRR) for  $^1\text{H}$  and  $^2\text{H}$  hydrogen-transfer reactions as a function of the atomic charge on the hydrogen atom, at 373 K. (7a)  $\text{R} = \text{F}$ ,  $\text{R}^1 = \text{H}$ ; (7b)  $\text{R} = \text{R}^1 = \text{H}$ ; (7c)  $\text{R} = \text{H}$ ,  $\text{R}^1 = \text{F}$

no correlation between the symmetry of the transition state and the value of HRR, the most symmetrical (7,  $\text{R} = \text{R}^1 = \text{H}$ ) showing an intermediate value for the calculated isotope effect. The largest calculated values of HRR are for (12) and (22), which correspond not to concerted hydrogen transfers, but to C-H bond homolyses. There does appear to be some correlation between HRR and the calculated charge on the migrating hydrogen (Figure 9). The transition states corresponding to  $\text{H}^-$  transfers have a remarkably constant calculated charge on the hydrogen ( $-0.305 \pm 0.002$ ) and relatively low isotope effects, whilst the proton transfers between oxygen (14, 15, and 18) show consistently higher values for HRR.

Using  $\text{R} = \text{R}^1 = \text{H}$  as a model, the MNDO calculations show that the lowest predicted KIE is for hydride transfer [Figure 1, path (a)], but that the magnitude (Table 3) is significantly greater than that observed for the Cannizzaro reaction of benzaldehyde ( $k^1\text{H}/k^2\text{H}_{373} \leq 1.8$ ). The only mechanism excluded from this comparison is the one involving a single-electron transfer [Figure 1, path (b)], since the UHF SCF method cannot be used for the calculation of excited states (*vide supra*). The calculations do indicate that with a more realistic model for the benzaldehyde reaction ( $\text{R} = \text{R}^1 = \text{Ph}$  rather than H), such a mechanistic pathway may be energetically more competitive with the other mechanisms discussed in this paper. The relatively poor agreement between the calculated KIE for these other mechanisms (for  $\text{R} = \text{R}^1 = \text{H}$ ) and experiment may indicate that the observed results for

benzaldehyde contain a significant contribution from such an electron-transfer mechanism. This mechanism is predicted to be less favourable for aliphatic aldehydes, which implies that hydrogen KIE for such aldehydes should be significantly larger than for benzaldehyde.

### Conclusions

The MNDO calculations reported in this paper suggest that, in the absence of significant effects due to preferential solvation, a hydride-ion transfer or a radical chain mechanism is clearly more favourable than a single-electron transfer (SET) or cyclic mechanism for the Cannizzaro reaction of aliphatic aldehydes. For aromatic aldehydes ( $\text{R} = \text{R}^1 = \text{Ph}$ ), the SET mechanism is predicted to be significantly more competitive with the hydride transfer. At high pH, a different mechanism is predicted for aliphatic aldehydes, implying the intermediate formation of hydrogen atoms.

### References

- 1 T. A. Geissman, *Org. React.*, 1944, **2**, 94.
- 2 F. Haber and R. Willstätter, *Chem. Ber.*, 1931, **64**, 2851; J. Weiss, *Trans. Faraday Soc.*, 1941, **37**, 782.
- 3 E. R. Alexander, *J. Am. Chem. Soc.*, 1947, **69**, 289.
- 4 (a) C. G. Swain, A. L. Powell, W. A. Sheppard, and C. R. Morgan, *J. Am. Chem. Soc.*, 1979, **101**, 3576; (b) C. G. Swain, A. L. Powell, T. J. Lynch, S. R. Alpha, and R. P. Dunlap, *ibid.*, p. 3584.
- 5 S. K. Chung, *J. Chem. Soc., Chem. Commun.*, 1982, 480.
- 6 E. C. Ashby, D. T. Coleman, and M. P. Gamasa, *Tetrahedron Lett.*, 1983, **24**, 851.
- 7 M. J. S. Dewar and W. Thiel, *J. Am. Chem. Soc.*, 1977, **99**, 4899, 4908; M. J. S. Dewar and M. L. McKee, *ibid.*, p. 5841; M. J. Dewar and H. S. Rzepa, *ibid.*, 1978, **100**, 58, 777; M. J. S. Dewar, M. L. McKee, and H. S. Rzepa, *ibid.*, p. 3607; L. P. Davis, R. M. Guidry, J. R. Williams, M. J. S. Dewar, and H. S. Rzepa, *J. Comput. Chem.*, 1981, **2**, 433; M. J. S. Dewar and H. S. Rzepa, *ibid.*, 1983, **4**, 158; M. J. S. Dewar and M. L. McKee, *ibid.*, p. 4, 82.
- 8 (a) S. B. Brown, M. J. S. Dewar, G. P. Ford, D. J. Nelson, and H. S. Rzepa, *J. Am. Chem. Soc.*, 1978, **100**, 7832; (b) H. S. Rzepa, *J. Chem. Soc., Chem. Commun.*, 1981, 939; (c) B. Anhede, N. A. Bergman, and L. Melander, *Acta Chem. Scand., Ser. A*, 1983, **37**, 843; (d) J. P. Shea, S. D. Nelson, and G. P. Ford, *J. Am. Chem. Soc.*, 1983, **105**, 5451.
- 9 M. J. S. Dewar, S. Olivella, and H. S. Rzepa, *Chem. Phys. Lett.*, 1977, **47**, 80.
- 10 P. K. Weiner, Ph.D. Dissertation, University of Texas, Austin, 1974.
- 11 M. J. S. Dewar, G. P. Ford, M. L. McKee, H. S. Rzepa, W. Thiel, and Y. Yamaguchi, *J. Mol. Struct.*, 1978, **43**, 435.
- 12 M. L. Steigerwald, W. A. Goddard, and D. A. Evans, *J. Am. Chem. Soc.*, 1979, **101**, 1944.
- 13 G. A. Craze and I. Watt, *J. Chem. Soc., Perkin Trans. 2*, 1981, 175.
- 14 M. M. Kreevoy and I. H. Lee, *J. Am. Chem. Soc.*, 1984, **106**, 2550.
- 15 M. J. S. Dewar and H. S. Rzepa, *J. Am. Chem. Soc.*, 1978, **100**, 784.
- 16 A. Albert and E. P. Serjeant, 'The Determination of Ionisation Constants,' Chapman and Hall, London, 1974, p. 86.
- 17 F. H. Westheimer, *Chem. Rev.*, 1961, **61**, 265; see also M. Wolfsberg, *Annu. Rev. Phys. Chem.*, 1969, 449.

Received 20th July 1984; Paper 4/1254